ACCOUNTS of chemical research

pubs.acs.org/accounts Article

Genetically Encoded Photocatalysis for Spatiotemporally Resolved Mapping of Biomolecules in Living Cells and Animals

Published as part of Accounts of Chemical Research special issue "Proximity-Induced Chemical Biology".

Yuxin Fang and Peng Zou*

Cite This: *Acc. Chem. Res.* 2025, 58, 2526−2534 Read Online

ACCESS | Metrics & More | Article Recommendations

CONSPECTUS: Engineered photosensitizer proteins, such as miniSOG, KillerRed, and SuperNova, have long been used for light-triggered protein inhibition and cell ablation. Compared to synthetic organic dyes, these genetically encoded tags provide superior spatial precision for subcellular targeting. More recently, the photochemistry of miniSOG has been repurposed for subcellular omics studies. Upon light activation, miniSOG generates reactive oxygen species (ROS) that oxidize nearby nucleic acids or proteins. These oxidized biomolecules can then react with exogenously supplied nucleophilic probes, which introduce bio-orthogonal handles for downstream enrichment and analysis.

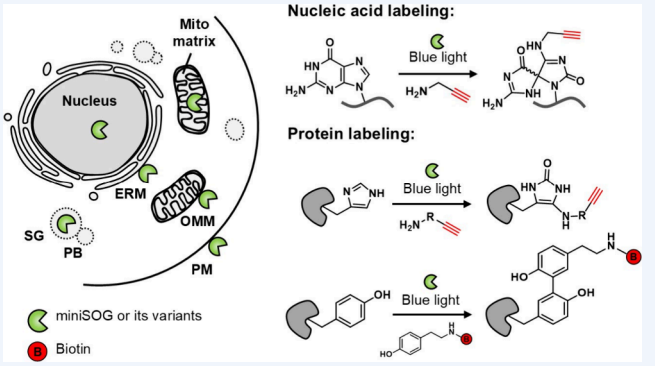

This labeling strategy, known as photocatalytic proximity labeling (PPL), has emerged as a powerful approach for profiling the molecular architecture of subcellular compartments and identifying RNA or protein interactors of specific targets. The use of light provides exceptional temporal control, enabling labeling windows as short as 1 s. Moreover, PPL readily supports pulse-chase experiments through simple light on/off switching, an advantage not easily achievable with conventional platforms such as APEX or TurboID.

In this account, we highlight our recent developments and applications of genetically encoded PPL tools. These include CAP-seq for RNA/DNA labeling, RinID for protein labeling, and LAP-seq/MS/CELL for bioluminescence-activated multi-omic profiling. Together, these tools enable detailed mapping of the cellular biomolecular landscape. For example, CAP-seq revealed enrichment of transcripts encoding secretory and mitochondrial proteins near the endoplasmic reticulum membrane and outer mitochondrial membrane, supporting models of localized translation. Additionally, pulse-chase labeling using RinID in the ER lumen uncovered distinct decay kinetics of secretory proteins.

Looking forward, future efforts may focus on developing low-toxicity and low-background chemical probes, engineering red-shifted photosensitizers for deep-tissue and *in vivo* applications, and integrating multiple proximity labeling (PL) platforms to study organelle contact sites and interorganelle molecular trafficking.

KEY REFERENCES

- Wang, P.; Tang, W.; Li, Z.; Zou, Z.; Zhou, Y.; Li, R.; Xiong, T.; Wang, J.; Zou, P. Mapping spatial transcriptome with light-activated proximity-dependent RNA labeling. *Nat. Chem. Biol.* **2019**, *15*, 1110−1119.[1] The first report of genetically encoded photocatalytic proximity labeling technique. CAP-seq enables light-activated RNA labeling with high spatial precision, allowing transcriptome mapping at subcellular resolution in living cells.
- Zheng, F.; Yu, C.; Zhou, X.; Zou, P. Genetically encoded photocatalytic protein labeling enables spatially-resolved profiling of intracellular proteome. *Nat. Commun.* **2023**, *14*, 2978.[2] Photocatalytic proximity labeling of subcellular proteomes. RinID utilizes genetically encoded flavin photocatalyst for light-triggered protein tagging, enabling spatially resolved proteomic profiling with high temporal control in living cells.
- Ren, Z.; Tang, W.; Peng, L.; Zou, P. Profiling stress-triggered RNA condensation with photocatalytic proximity labeling. *Nat. Commun.* **2023**, *14*, 7390.[3] Application of CAP-seq to investigate the transcriptome profiles of the membraneless organelle stress granule during its

Received: June 6, 2025
Revised: July 5, 2025
Accepted: July 8, 2025
Published: July 21, 2025

https://doi.org/10.1021/acs.accounts.5c00390
Acc. Chem. Res. 2025, 58, 2526−2534

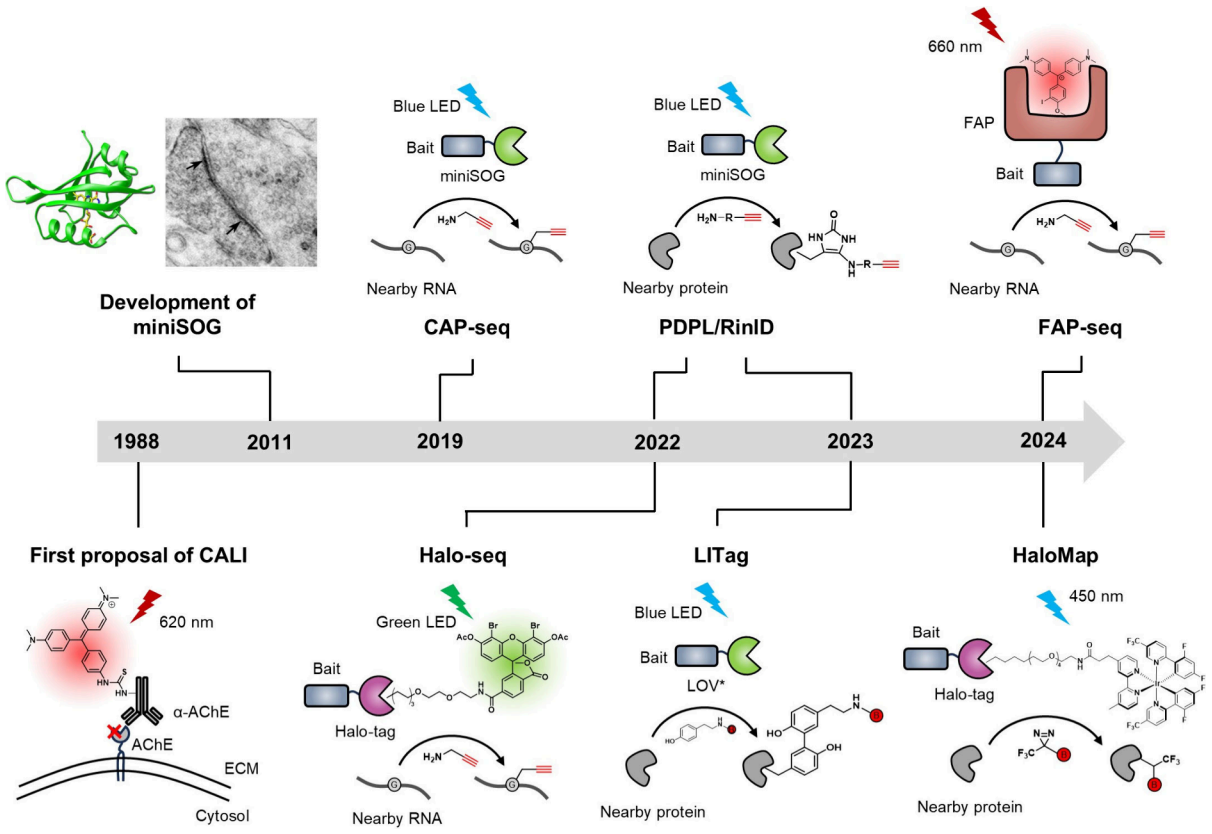

Figure 1. Milestones in the development of genetically encoded photocatalysis. The miniSOG structure and electron microscope image are reproduced with permission from ref 8. Copyright: 2011, PLOS.

assembly and disassembly stages. This study reveals dynamic RNA recruitment and release patterns under cellular stress with spatiotemporal resolution.

- Wang, R.; Fang, Y.; Hu, Y.; Liu, Y.; Chen, P. R.; Zou, P. Bioluminescence-activated proximity labeling for spatial multi-omics. *Chem.* **2025**, 102595.[4] Bioluminescence-activated spatial multiomic profiling. The LAP platform enables light-free proximity labeling of proteins, RNAs, and cell−cell interfaces via NanoLuc-driven photocatalysis, offering high-resolution, in vivo-compatible spatial omics mapping.

INTRODUCTION

Light offers unparalleled spatiotemporal control over chemical reactions, making it an ideal tool for probing and perturbing biological systems with subcellular precision. The therapeutic use of photoactive chemical reactions dates back over a century. In 1903, Niels Finsen was awarded the Nobel Prize for his pioneering work in phototherapy. Decades later, in 1988, Daniel Jay introduced the concept of chromophore-assisted laser inactivation (CALI) to inactivate specific proteins.[5] This was achieved by conjugating the organic dye malachite green to an antibody targeting acetylcholinesterase on the cell surface, enabling site-specific protein inactivation via laser irradiation. While CALI and other small molecule-based strategies have demonstrated effectiveness, their specific subcellular targeting often rely on antibodies, which are generally restricted to the cell surface due to their large size and membrane impermeability.

To overcome these challenges, genetically encoded photoactive proteins have emerged as powerful alternatives. Engineered proteins such as KillerRed,[6] SuperNova,[7] and miniSOG[8] can be genetically fused to intracellular targets and expressed in defined subcellular compartments. Upon light activation, these proteins mediate localized chemical reactions, including protein inactivation, reactive oxygen species (ROS) generation, and photooxidation, thus offering versatile means of spatially precise perturbation. These tools have significantly expanded the applications of light-induced manipulation, ranging from protein inactivation[9] and cell ablation[10] to correlated light and electron microscopy (CLEM)[8] and spatially resolved omics analyses[1−4,11−13] (Figure 1).

Among these, miniSOG is a flavin mononucleotide (FMN)-binding protein engineered from the light, oxygen, voltage (LOV) domain of *Arabidopsis thaliana* phototropin 2[8] (Figure 2A). Like FMN, miniSOG absorbs maximally at 448 nm and emits green fluorescence with peaks at 500 and 528 nm (Figure 2B). Upon blue light irradiation, FMN transitions from its excited singlet state (^{1}FMN*) to a reactive triplet state (^{3}FMN*) via intersystem crossing (ISC). This triplet state can undergo energy transfer to produce singlet oxygen or electron transfer to generate superoxide anions (Figure 2C). Initially developed to enhance contrast in electron microscope (EM) by catalyzing diaminobenzidine polymerization (Figure 2D), miniSOG was later employed for targeted photoablation of neurons[10] and inhibition of synaptic proteins in *Caenorhabditis elegans*[9] (Figure 2E-F), leveraging its capability to generate ROS.

In 2019, our laboratory introduced chromophore-assisted proximity labeling and sequencing (CAP-seq), a method that uses miniSOG to oxidize proximal RNAs upon light activation. This approach employed propargylamine (PA) as a primary amine probe to capture oxidative RNA adducts and enabled subsequent bio-orthogonal tagging and enrichment.[1] Building

https://doi.org/10.1021/acs.accounts.5c00390
Acc. Chem. Res. 2025, 58, 2526−2534

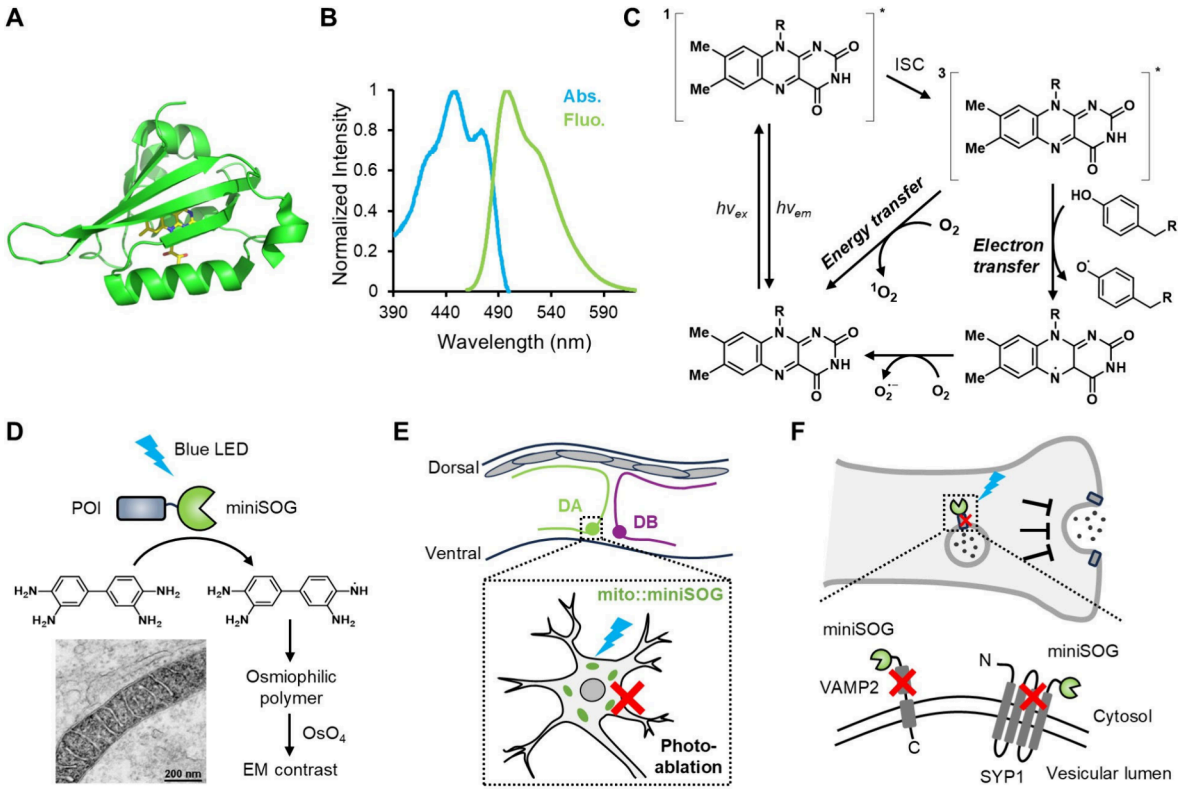

Figure 2. Development and initial applications of miniSOG. (A) Crystal structure of miniSOG (PDB: 6GPU). (B) Absorption (Abs.) and fluorescence (Fluo.) spectra of miniSOG. (C) Type I (electron transfer) and Type II (energy transfer) photoreaction mechanisms of FMN. In the electron transfer mechanism, electron-rich amino acids (e.g., tyrosine, tryptophan, histidine) can act as electron donors, as exemplified by tyrosine-to-triplet FMN electron transfer in the panel. (D) Mechanism of miniSOG-catalyzed photoreaction enhancing electron microscope (EM) contrast. The EM image showing mitochondrial targeted miniSOG is reproduced with permission from ref (8). Copyright: 2011, PLOS. (E–F) Schematic cartoon showing miniSOG-mediated selective ablation of dorsal A-type (DA) and B-type (DB) motor neurons in *C. elegans* (E) or chromophore-assisted light inactivation (CALI) of synaptic vesicle proteins (F).

on this initial effort, we and others have since developed a suite of photocatalytic proximity labeling (PPL) tools targeting both RNA and proteins, utilizing miniSOG alongside other photoactive proteins and small molecules[2,4,11−16] (Figure 1). In this Account, we provide a comprehensive overview of genetically encoded PPL systems based on miniSOG and its engineered variants.

PPL FOR TRANSCRIPTOMIC AND GENOMIC STUDIES

Nucleobases are known to undergo oxidation by ROS, with guanosine being the most susceptible among the four canonical bases.[17] Oxidative modification of guanosine yields products that can readily cross-link with amines.[18,19] To validate these chemical transformations, guanosine was subjected to blue light irradiation in the presence of miniSOG and subsequently analyzed by liquid chromatography coupled with tandem mass spectrometry (LC-MS/MS). Oxidized guanosine derivatives, including imidazolone and spiroiminodihydantoin, were detected as major products.

To enrich oxidized RNAs, a series of biotin-conjugated amine probes, including alkylamine, aniline, and alkoxyamine were evaluated under miniSOG-catalyzed photo-oxidation conditions. Among these, alkylamine exhibited the highest reactivity. The biotinylation signals were significantly reduced in the presence of sodium azide and enhanced in deuterium oxide (D_2O), indicating a singlet oxygen−dependent labeling mechanism. To improve probe permeability, the biotin moiety was replaced with a terminal alkyne, which served as a bioorthogonal enrichment handle.

In a typical CAP-seq labeling workflow, cells are incubated with PA for 5 min, followed by blue light irradiation for 15 min. After irradiation, cells are lysed, and total RNA is extracted and reacted with azide-conjugated biotin via click chemistry. The biotinylated RNAs are then enriched using streptavidin-coated beads and subsequently analyzed by next-generation sequencing (NGS) (Figure 3A). As a proof of concept, miniSOG was first targeted to the mitochondrial matrix in human embryonic kidney 293T (HEK293T) cells. CAP-seq at this location led to the enrichment of all 13 mitochondrial-encoded mRNAs and both mitochondrial rRNAs.

To extend the approach to membrane-associated transcriptomes, miniSOG was localized to the endoplasmic reticulum membrane (ERM) and the outer mitochondrial membrane (OMM).[1] CAP-seq at the ERM enriched 372 mRNAs and 5 noncoding RNAs, 96.2% of which encoded secretory proteins. These data are consistent with the model of localized protein translation at the ER, where secretory proteins are synthesized and cotranslationally translocated into the ER lumen (Figure 3B). CAP-seq at the OMM identified 411 mRNAs and 61 noncoding RNAs, including 110 mRNAs encoding mitochondrial proteins, of which 53 corresponded to inner mitochondrial membrane (IMM) components. Notably, 55 mRNAs encoding cytoplasmic ribosomal subunits were also enriched at the OMM (Figure 3C), suggesting that the OMM-proximal transcriptome is more complex than that of ERM, and

https://doi.org/10.1021/acs.accounts.5c00390
Acc. Chem. Res. 2025, 58, 2526−2534

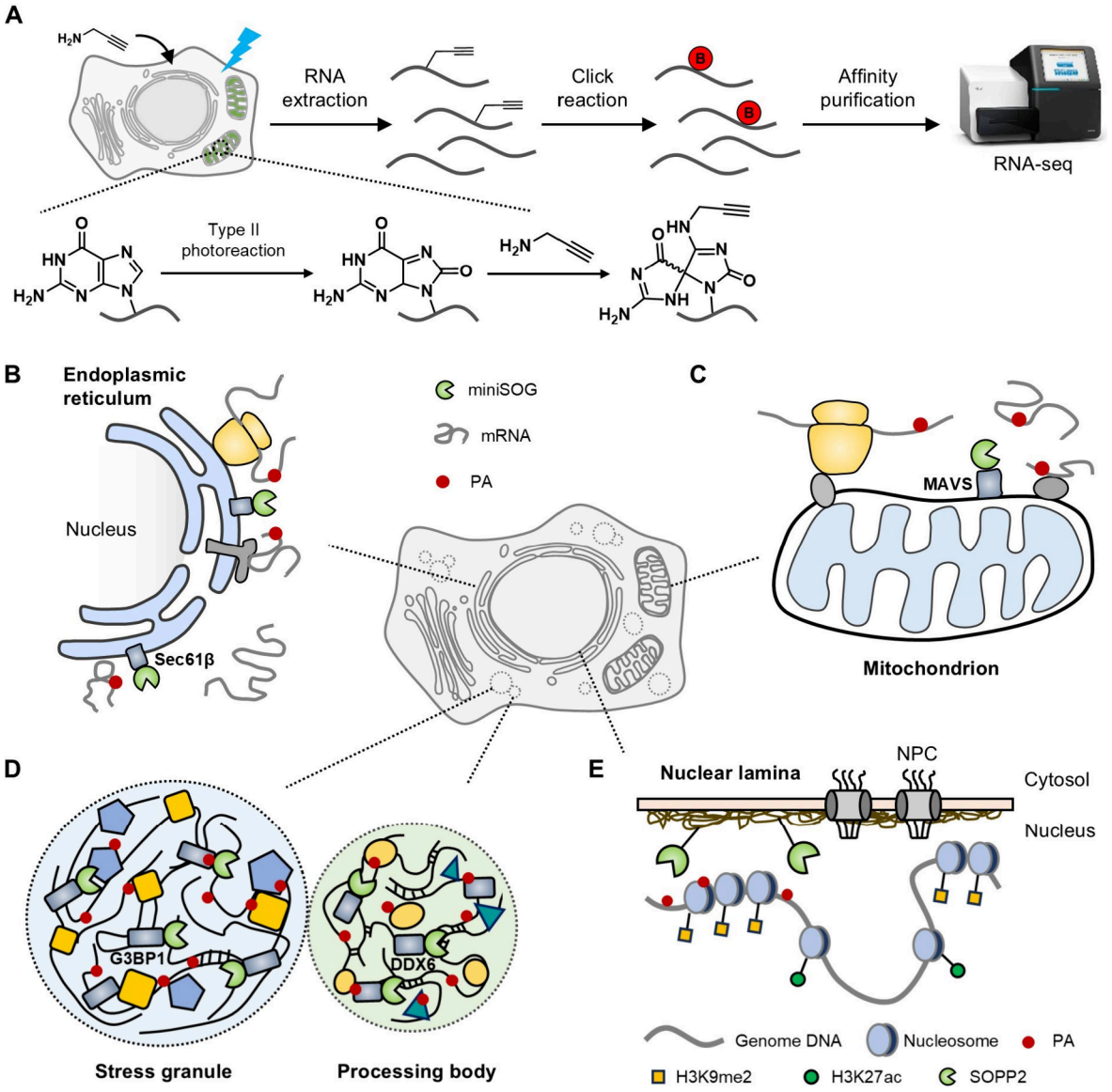

Figure 3. PPL for transcriptomic and genomic studies. (A) Workflow of CAP-seq. The labeling reaction was initiated by blue light irradiation in the presence of propargylamine (PA) probe. Following the irradiation, total RNAs were extracted, conjugated with azide-biotin, and affinity purified with streptavidin-coated magnetic beads, and analyzed by sequencing. (B) Sec61β-fused miniSOG mapped the ERM-proximal transcriptome. (C) MAVS C-terminal domain-fused miniSOG mapped the OMM-proximal transcriptome. (D) G3BP1- and DDX6-fused miniSOG mapped the stress granule and processing body transcriptome, respectively. (E) Lamin A-fused miniSOG mapped the lamina-proximal chromatin.

comprises components beyond just locally translated transcripts.

More recently, CAP-seq was used to profile the transcriptomes of membraneless organelles, including stress granules (SGs) and processing bodies (PBs)[20] (Figure 3D). To investigate SG-associated RNAs, miniSOG was fused to the scaffold protein G3BP1 and expressed in cells under basal conditions, oxidative stress, and recovery following stress withdrawal. CAP-seq data revealed a preferential enrichment of long, AU-rich transcripts in SGs, with these features persisting even after stress removal. To study PB-associated RNAs, miniSOG was fused to the N-terminus of the PB marker DDX6. CAP-seq identified 179 and 563 enriched transcripts under basal and arsenite-treated conditions, respectively. Compared to transcripts in basal PBs, stress-recruited mRNAs showed no significant changes in transcript length, including coding sequence (CDS) and untranslated regions (UTRs), but exhibited higher AU content in both the CDS and 3′ UTR.

The CAP-seq strategy was also adapted for DNA labeling.[11] Despite challenges posed by the low abundance and double-stranded structure of DNA, successful DNA tagging was achieved by replacing miniSOG with SOPP2, an engineered variant with a higher quantum yield of singlet oxygen. When SOPP2 was targeted to the nuclear lamina in HEK293T cells, lamina-associated chromatin regions were identified, overlapping with heterochromatic markers such as histone H3 lysine 9 dimethylation (Figure 3E).

PPL FOR PROTEOMIC STUDIES

Between 2022 and 2023, protein labeling via miniSOG-mediated photocatalysis was independently reported by Gang Li's group (PDPL, 2022),[12] Tom W. Muir's group (LITag, 2023),[13] and our laboratory (RinID, 2023).[2] In these studies,

https://doi.org/10.1021/acs.accounts.5c00390
Acc. Chem. Res. 2025, 58, 2526−2534

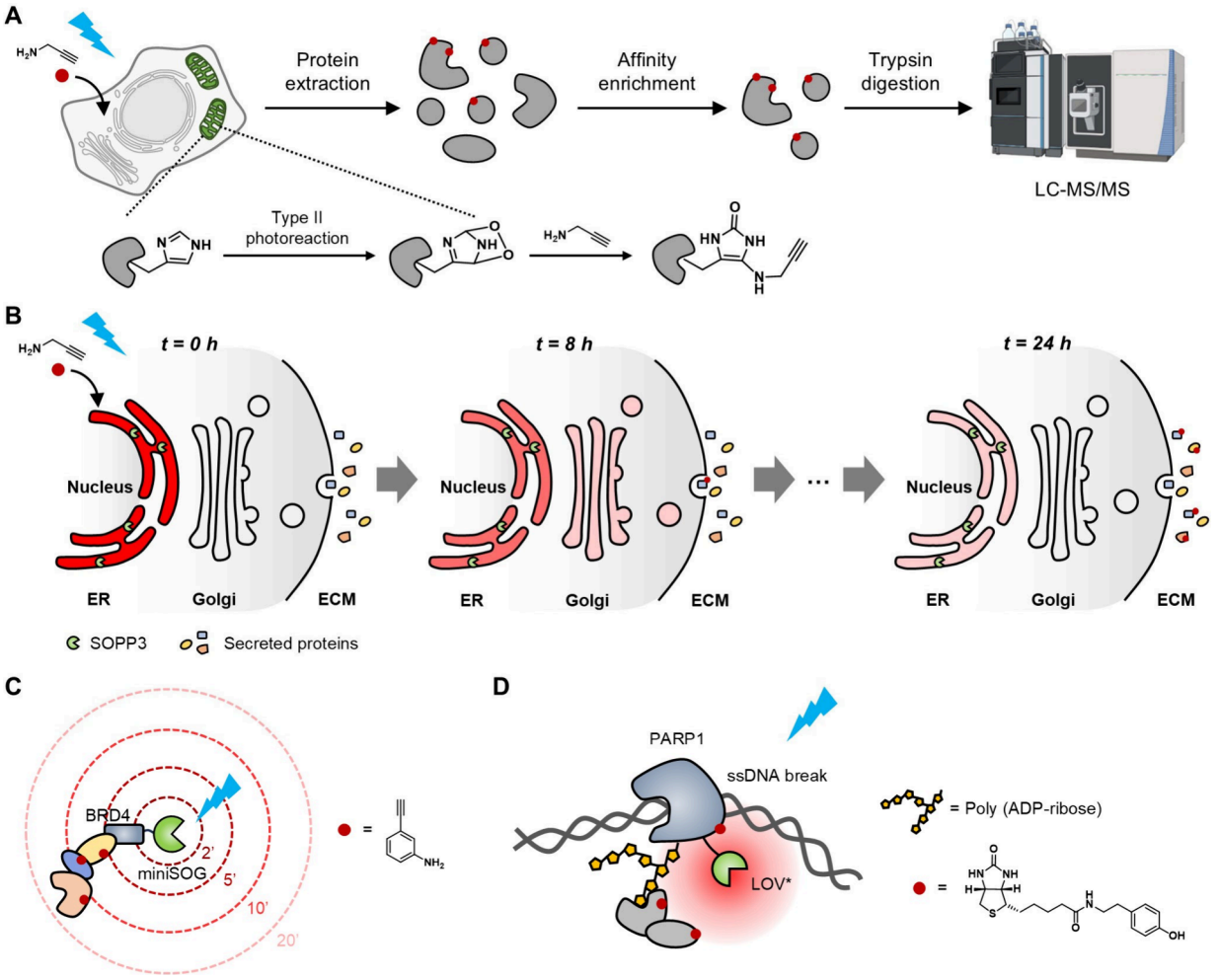

Figure 4. PPL for proteomic studies. (A) Workflow of RinID. The labeling reaction was initiated by blue light irradiation in the presence of PA probe. Following the irradiation, proteins were extracted, conjugated with azide-biotin, and affinity purified with streptavidin-coated agarose beads, digested with trypsin and analyzed by LC-MS/MS. (B) Pulse-chase labeling with miniSOG to determine the clearance rate of ER lumen proteins. RinID labeling was performed at $t = 0$ h, then the cells were washed and cultured for 8, 16, or 24 h. Protein extracted from four time points were enriched with streptavidin-coated beads and analyzed by TMT-based quantitative MS. ECM, extracellular matrix. (C) BRD4-fused miniSOG mapped disease-associated interactors with 2−20 min of irradiation. (D) PARP1-fused LOV* mapped the interactome of PARylation.

nucleophilic probes were employed to capture photo-oxidized proteins (e.g., alkylamine in RinID and aniline in PDPL) using a mechanism analogous to that of RNA labeling in CAP-seq. LC-MS/MS analysis confirmed that histidine residues served as the primary labeling sites, where adducts were formed between the amine probes and the C4 position of 2-oxo-imidazole, the oxidation product of histidine (Figure 4A). In contrast, LITag employed a biotin-phenol (BP) probe that underwent electron transfer upon blue light irradiation, generating phenoxy radicals capable of cross-linking to nearby tyrosine residues. To improve temporal precision, a miniSOG mutant (LOV*) and a high-intensity blue LED source (450 mW/cm^2) were used, allowing efficient labeling with only one second of irradiation.

One of the key advantages of genetically encoded PPL is the ability to precisely control the timing of labeling. Owing to this temporal resolution and its good biocompatibility, PPL has been applied to pulse-chase experiments for studying protein turnover. A pulse-chase labeling experiment was designed in HeLa cells stably expressing SOPP3 anchored in the ER lumen. The RinID labeling procedure was conducted at time zero, followed by washing to remove excess probe. Cells were then cultured for 8, 16, and 24 h. Quantitative proteomic analysis was performed using a 10-plex tandem mass tag (TMT) labeling strategy to assess the dynamics of biotinylated proteins. Secreted proteins were found to exhibit significantly faster turnover than ER-resident proteins. Notably, TGM2 and LIPL displayed rapid clearance, with signal intensities reduced by 73% and 51%, respectively, after an 8-h chase period (Figure 4B).

In PDPL, miniSOG was fused to the transcriptional coactivator BRD4 and the E3 ubiquitin ligase Parkin to map their protein interaction networks. To modulate the labeling radius, cells expressing BRD4 miniSOG fusions were irradiated with blue light for varying durations (2−20 min), resulting in progressively increased labeling of protein interactors (Figure 4C). In LITag, LOV* was targeted to poly(ADP-ribose) polymerase 1 (PARP1) and major vault protein (MVP) for interactome profiling. Proteomic analysis of PARP1-associated proteins identified HMGB1 as a PARylation-dependent interactor, whose recruitment to DNA damage sites was shown to be PARP1-dependent (Figure 4D). For MVP, the labeled interactome revealed associations with nuclear transport factors and protein-folding chaperones, supporting the proposed roles of vault particles in nuclear trafficking and protein quality control.

https://doi.org/10.1021/acs.accounts.5c00390
Acc. Chem. Res. 2025, 58, 2526−2534

Table 1. Comparison of Different PPL Platforms for Proteomic Studies

	RinID[2]	PDPL[12]	LITag[13]
PPL tag	miniSOG/SOPP3	miniSOG	LOV* (a.k.a. SOPP)
probe	propargylamine	3-ethylaniline	biotin-phenol/aniline
irradiation condition	30 mW/cm^2, 5−15 min	10 W LED, 2−20 min	450 mW/cm^2, 1−3 s

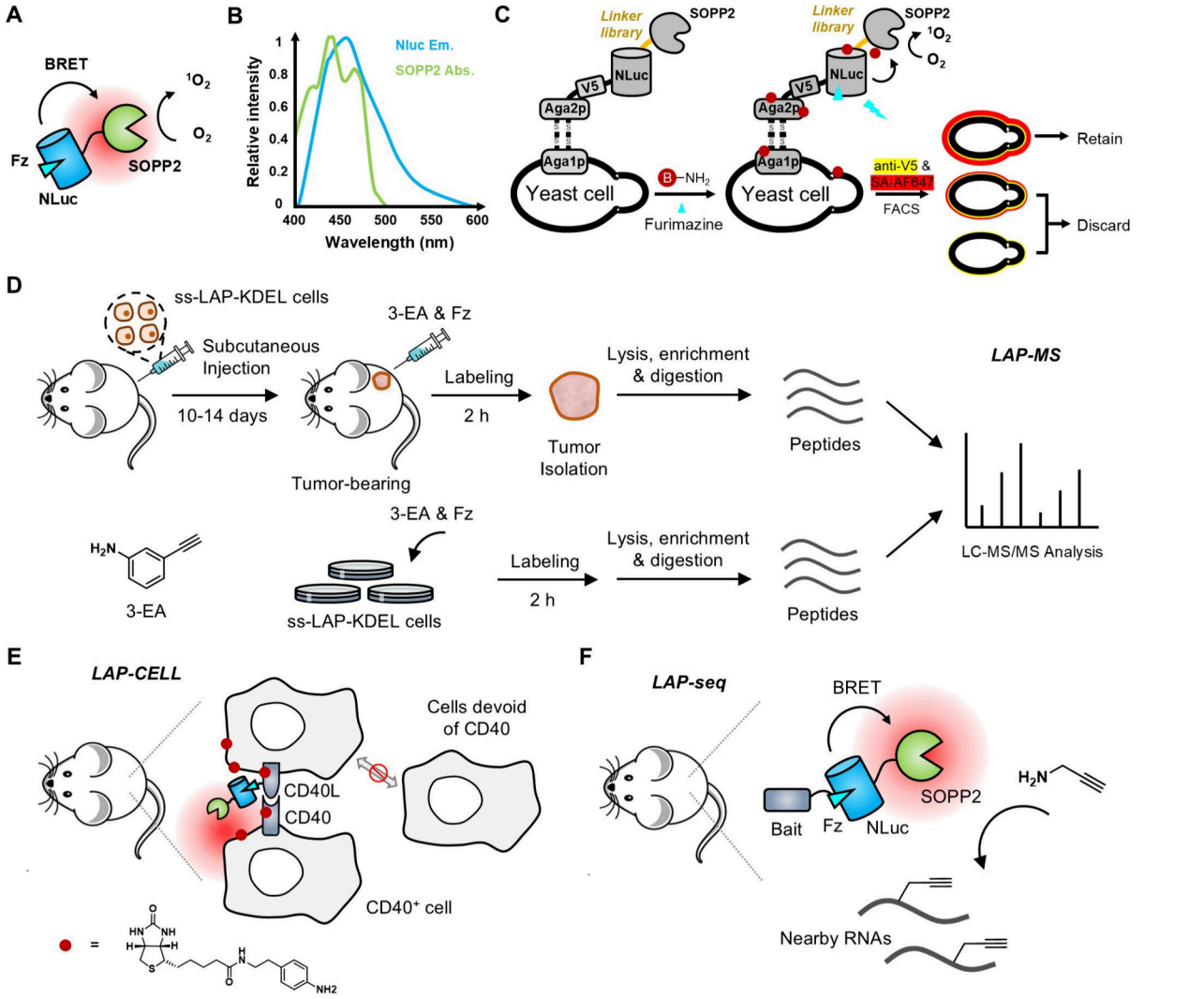

Figure 5. Design, engineering, and applications of LAP. (A) Design of the LAP strategy. Fz, furimazine. (B) Schematic showing the overlap between the emission spectrum of NanoLuc (NLuc Em.) and the absorption spectrum of SOPP2 (SOPP2 Abs.). (C) Schematic showing the selection of flexible linkers between NanoLuc and SOPP2 using yeast display. (D) Comparison of the secretory proteome between cultured cancer cells and implanted tumors using LAP-MS. (E) CD40L-fused LAP selectively labeled interacting cells expressing CD40 in living mice. (F) Sec61β-fused LAP mapped the ERM-proximal transcriptome in living mice.

The development of RinID, PDPL, and LITag highlights the robust protein-labeling capabilities of miniSOG and its variants. As noted by Hanaya et al.,[13] amine-based probes, which operate via an energy transfer mechanism, offer higher labeling efficiency but also result in increased background signals. In contrast, phenol-based probes, which rely on an electron transfer mechanism, produce cleaner backgrounds but with lower labeling intensity. The differences among these three platforms are illustrated in Table 1. The choice of proximity labeling enzymes, probe types, and irradiation conditions can be tailored to suit specific experimental needs.

BRET-BASED PPL FOR MULTIOMIC STUDIES IN LIVING ANIMALS

Although light-activated PL offers high spatiotemporal resolution, the limited tissue penetration of blue light has restricted its application in living animals. To overcome this limitation, a luminescence-activated proximity labeling (LAP) strategy was developed by fusing miniSOG with NanoLuc, a luciferase engineered from *Oplophorus gracilirostris*[4,21] (Figure 5A). The emission spectrum of NanoLuc (λ_{max} = 460 nm) was found to overlap closely with the absorption spectra of miniSOG (λ_{max} = 450 nm) and its variants, such as SOPPs (λ_{max} = 440 nm) (Figure 5B). This spectral compatibility, along with the small molecular sizes of both NanoLuc (~3 nm) and miniSOG (~2

https://doi.org/10.1021/acs.accounts.5c00390
Acc. Chem. Res. 2025, 58, 2526−2534

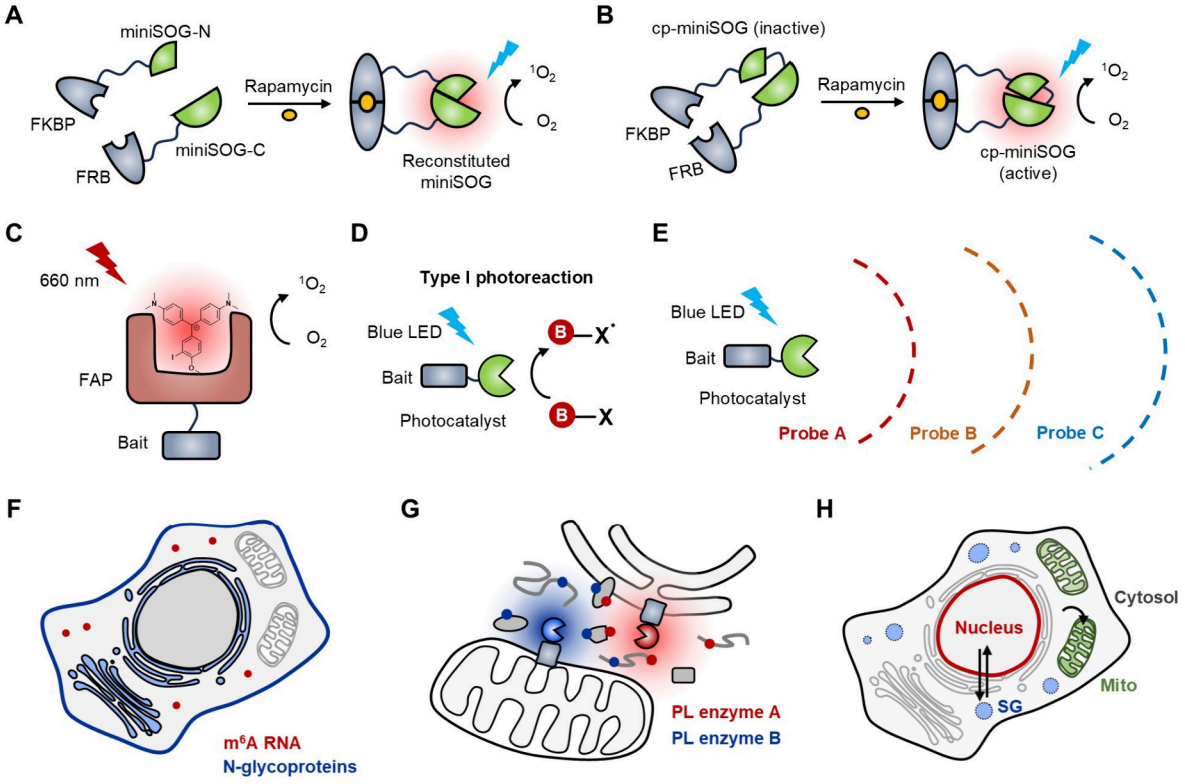

Figure 6. Future directions for PPL technology development. (A) Split-miniSOG reconstruction using the rapamycin-dependent FKBP-FRB dimerization system. (B) Activity reconstitution of circularly permutated miniSOG using the rapamycin-dependent FKRP-FRB dimerization system. (C) NIR-light activated PL with malachite-green binding fluorogen-activating protein (FAP). (D) PPL via the type I photoreaction. (E) Spatially multiscaled PPL with diverse chemical probes. (F) Asymmetrical distribution of N-glycoproteins and m^{6}A RNAs in eukaryotic cells. (G) Orthogonal labeling with different PL technologies for investigating components of organelle contact sites. (H) Sequential labeling with different PL technologies for investigating the protein trafficking between organelles.

nm), enabled efficient bioluminescence resonance energy transfer (BRET). The Förster radius for the NanoLuc-miniSOG pair was estimated to be approximately 3.7 nm, indicating that BRET efficiency would be highly sensitive to the donor−acceptor distance.

To enhance labeling efficiency, a SOPP2 mutant (I34V/I55V), previously evolved through yeast surface display, was incorporated and shown to yield stronger labeling than the parent SOPP2 on both yeast and HEK293T cell surfaces. Multiple LAP fusion constructs were subsequently engineered by 1) fusing NanoLuc to either the N- or C-terminus of SOPP2$^{I34V/I55V}$, 2) varying linker lengths, and 3) randomizing linker sequences. A library comprising over 3×10^6 constructs was screened via yeast display (Figure 5C). From this screen, an optimized construct was identified that exhibited 1.95-fold and 4.80-fold enhanced labeling on yeast and HEK293T surfaces, respectively, compared to the initial SOPP2$^{I34V/I55V}$-NanoLuc fusion. Structural prediction using AlphaFold3 estimated the donor−acceptor distance in the final LAP construct to be 3.2 nm, well within the Förster radius for effective BRET.

This engineered LAP system enabled subcellular proteomic profiling (LAP-MS) in live animal models (Figure 5D). MC38 cells stably expressing ER lumen-targeted LAP were subcutaneously implanted into mice to form solid tumors. Following approximately 2 weeks of tumor growth, a labeling reaction was initiated by intratumoral injection of a 3-EA and furimazine mixture. In parallel, the labeling was also performed on MC38 cell culture *in vitro*. Comparison of the ER lumen proteomes between cultured cells and tumor tissues revealed a reduced representation of ER-resident proteins and an increased proportion of extracellular and membrane proteins in tumors, suggesting that these secreted proteins may contribute to tumor development and progression.

The LAP strategy was also adapted to map cell−cell communications (LAP-CELL) and subcellular transcriptome profiling (LAP-seq). For LAP-CELL, a biotin-conjugated aniline probe was used to label surface proteins. After labeling, cells were dissociated, stained with streptavidin-conjugated fluorescent dyes, and analyzed by flow cytometry. In a CD40-CD40L interaction model, substantial trans-biotinylation of CD40-expressing cells was observed when cocultured with CD40L-LAP cells, whereas GFP-expressing control cells exhibited negligible labeling, confirming the efficiency and specificity of LAP-CELL *in vivo* (Figure 5E).

For transcriptomic applications (LAP-seq), LAP constructs were targeted to the ERM in HEK293T and MC38 cells, and labeling was conducted by incubating cells with PA and furimazine for 1 h. The resulting ERM-proximal transcriptome displayed secretory enrichment comparable to that obtained by CAP-seq, with broader transcript coverage. *In vivo* compatibility of LAP-seq was further validated in tumor-bearing mice, where enrichment of the secretory gene *CANX* was confirmed by RT-qPCR (Figure 5F).

CONCLUSION AND PERSPECTIVES

In summary, genetically encoded PPL offers precise temporal and spatial control for subcellular multi-omic studies. Compared to small-molecule photocatalysts, protein-based photocatalysts

https://doi.org/10.1021/acs.accounts.5c00390
Acc. Chem. Res. 2025, 58, 2526−2534

provide superior subcellular targeting convenience and specificity. Our miniSOG-mediated labeling strategy, has proved its efficiency and spatial specificity across various subcellular localizations. The BRET-based labeling tool suite, LAP-seq, LAP-MS, and LAP-CELL, has been demonstrated to be compatible with *in vivo* applications, enabling comprehensive characterization of local microenvironments in live animal models. Despite recent advancements that have significantly diversified the genetically encoded PPL toolkit, unmet needs persist in biological applications, necessitating the development of novel enzymes, innovative chemistry, and combinations of existing PPL platforms with other omic technologies.

Split PL enzymes, such as split-APEX2[22] and split-TurboID,[23] consist of inactive protein fragments that reconstitute into an active enzyme when physically colocalized, allowing the investigation of organelle contact sites and protein−protein interactions (PPIs). Circular permutation, which involves fusing the N- and C-termini of an enzyme with a flexible linker and creating new termini within the protein structure, results in an enzyme that is sensitive to conformational changes. Previous developments of split-miniSOG and circularly permutated LOV2 domains have been applied in EM imaging[24] and optogenetic manipulation,[25] respectively. However, the RNA and protein labeling capabilities of these enzymes have not yet been demonstrated, and further engineering is required to optimize their activity. We reasoned that engineering split-miniSOG (Figure 6A) and circularly permutated miniSOG (cp-miniSOG) (Figure 6B) could substantially advance multi-omic studies of protein−protein interactions.

While the LAP strategy has proven feasible for in vivo applications, it was observed that the labeling signals were much weaker compared to those from blue-light-activated methods. To address the tissue penetration issue, PPL enzymes with red-shifted spectra could serve as a promising alternative. Recently, Ying Li's group reported an RNA proximity labeling platform activated by near-infrared (NIR) light, utilizing a genetically encoded fluorogen-activating protein (FAP) that binds to malachite green derivatives.[15] Given the superior tissue penetration of NIR light, FAP-based PPL holds great potential for transcriptomic and proteomic profiling in living animals (Figure 6C).

Beyond innovations in enzyme engineering, the development of new chemical reactions is another critical future direction. The widely used type II photoreaction mechanism requires high concentrations of amine probes, which not only cause cytotoxicity but also result in background labeling of endogenous oxidative damage on proteins and RNAs. Building on the single-electron transfer (SET) mechanism employed by LITag, it is expected that other electron-rich chemicals may be oxidized by flavin to generate reactive radicals for proximity labeling (Figure 6D). Furthermore, diverse chemistries for PPL enable fine-tuning of the labeling radius based on the half-lives of various reactive intermediates (Figure 6E), as recently demonstrated by MultiMAP, a PPL platform for cell surface labeling using antibody-conjugated Eosin Y.[26]

Finally, PPL platforms can be integrated with other omic technologies to enable the characterization of local compartments across multiple dimensions simultaneously. For example, a recently developed photoactivated APEX2 labeling strategy leverages hydrogen peroxide generated by SOPP3 under blue light illumination in the presence of endogenous superoxide dismutase.[27] This SOPP3-APEX2 system eliminates the need for exogenous hydrogen peroxide, thereby reducing cytotoxicity, and shows strong potential for investigating organelle contact sites. Moreover, combining PPL with protein or RNA modification identification methods could provide valuable insights into the asymmetrical distribution of protein post-translational modifications (e.g., phosphorylation and glycosylation) or RNA epigenetic modifications such as N^6-methyladenosine (m^6A) (Figure 6F). Additionally, as exemplified by OrthoID[28] and TransitID,[29] PPL methods can be combined with other PL platforms to enable orthogonal labeling for profiling organelle contact sites (Figure 6G) or successive labeling to investigate protein and RNA trafficking between subcellular compartments (Figure 6H).

AUTHOR INFORMATION

Corresponding Author

Peng Zou − *College of Chemistry and Molecular Engineering, Synthetic and Functional Biomolecules Center, Beijing National Laboratory for Molecular Sciences, Key Laboratory of Bioorganic Chemistry and Molecular Engineering of Ministry of Education, PKU-IDG/McGovern Institute for Brain Research, Peking University, Beijing 100871, China; Academy for Advanced Interdisciplinary Studies, Peking-Tsinghua Center for Life Sciences and Beijing Advanced Center of RNA Biology (BEACON), Peking University, Beijing 100871, China; Chinese Institute for Brain Research (CIBR), Beijing 102206, China;* orcid.org/0000-0002-9798-5242; Email: zoupeng@pku.edu.cn

Author

Yuxin Fang − *College of Chemistry and Molecular Engineering, Synthetic and Functional Biomolecules Center, Beijing National Laboratory for Molecular Sciences, Key Laboratory of Bioorganic Chemistry and Molecular Engineering of Ministry of Education, PKU-IDG/McGovern Institute for Brain Research, Peking University, Beijing 100871, China*

Complete contact information is available at: https://pubs.acs.org/10.1021/acs.accounts.5c00390

Notes

The authors declare no competing financial interest.

Biographies

Yuxin Fang received her Ph.D. in Chemical Biology from Peking University in 2022. She is currently a postdoctoral fellow at the College of Chemistry and Molecular Engineering, Peking University. Her research interest lies in protein engineering and nucleic acid modifications. Her current research project focuses on developing novel photocatalytic proximity labeling tools via directed evolution.

Peng Zou completed his Ph.D. from Massachusetts Institute of Technology in 2012. Following his postdoctoral training at Harvard University, he joined Peking University in 2015 as an assistant professor in the College of Chemistry and Molecular Engineering and was promoted to associate professor with tenure in 2021. His research focuses on inventing chemical tools for the high-resolution mapping of biomolecules and biophysical signaling that underlie neuronal functions.

ACKNOWLEDGMENTS

This work was supported by the Ministry of Science and Technology (2022YFA1304700), the National Natural Science Foundation of China (32088101), and Beijing National

Laboratory for Molecular Sciences (BNLMS-CXXM-202403). P.Z. is sponsored by Bayer Investigator Award.

REFERENCES

(1) Wang, P.; Tang, W.; Li, Z.; Zou, Z.; Zhou, Y.; Li, R.; Xiong, T.; Wang, J.; Zou, P. Mapping spatial transcriptome with light-activated proximity-dependent RNA labeling. *Nat. Chem. Biol.* **2019**, *15*, 1110−1119.
(2) Zheng, F.; Yu, C.; Zhou, X.; Zou, P. Genetically encoded photocatalytic protein labeling enables spatially-resolved profiling of intracellular proteome. *Nat. Commun.* **2023**, *14*, 2978.
(3) Ren, Z.; Tang, W.; Peng, L.; Zou, P. Profiling stress-triggered RNA condensation with photocatalytic proximity labeling. *Nat. Commun.* **2023**, *14*, 7390.
(4) Wang, R.; Fang, Y.; Hu, Y.; Liu, Y.; Chen, P. R.; Zou, P. Bioluminescence-activated proximity labeling for spatial multi-omics. *Chem.* **2025**, 102595.
(5) Jay, D. G. Selective destruction of protein function by chromophore-assisted laser inactivation. *Proc. Natl. Acad. Sci. U. S. A.* **1988**, *85*, 5454−5458.
(6) Bulina, M. E.; Chudakov, D. M.; Britanova, O. V.; Yanushevich, Y. G.; Staroverov, D. B.; Chepurnykh, T. V.; Merzlyak, E. M.; Shkrob, M. A.; Lukyanov, S.; Lukyanov, K. A. A genetically encoded photosensitizer. *Nat. Biotechnol.* **2006**, *24*, 95−99.
(7) Takemoto, K.; Matsuda, T.; Sakai, N.; Fu, D.; Noda, M.; Uchiyama, S.; Kotera, I.; Arai, Y.; Horiuchi, M.; Fukui, K.; Ayabe, T.; Inagaki, F.; Suzuki, H.; Nagai, T. SuperNova, a monomeric photosensitizing fluorescent protein for chromophore-assisted light inactivation. *Sci. Rep* **2013**, *3*, 2629.
(8) Shu, X.; Lev-Ram, V.; Deerinck, T. J.; Qi, Y.; Ramko, E. B.; Davidson, M. W.; Jin, Y.; Ellisman, M. H.; Tsien, R. Y. A genetically encoded tag for correlated light and electron microscopy of intact cells, tissues, and organisms. *PLoS Biol.* **2011**, *9*, No. e1001041.
(9) Lin, J. Y.; Sann, S. B.; Zhou, K.; Nabavi, S.; Proulx, C. D.; Malinow, R.; Jin, Y.; Tsien, R. Y. Optogenetic inhibition of synaptic release with chromophore-assisted light inactivation (CALI). *Neuron* **2013**, *79*, 241−253.
(10) Qi, Y. B.; Garren, E. J.; Shu, X.; Tsien, R. Y.; Jin, Y. Photoinducible cell ablation in Caenorhabditis elegans using the genetically encoded singlet oxygen generating protein miniSOG. *Proc. Natl. Acad. Sci. U. S. A.* **2012**, *109*, 7499−7504.
(11) Ding, T.; Zhu, L.; Fang, Y.; Liu, Y.; Tang, W.; Zou, P. Chromophore-Assisted Proximity Labeling of DNA Reveals Chromosomal Organization in Living Cells. *Angew. Chem., Int. Ed. Engl.* **2020**, *59*, 22933−22937.
(12) Zhai, Y.; Huang, X.; Zhang, K.; Huang, Y.; Jiang, Y.; Cui, J.; Zhang, Z.; Chiu, C. K. C.; Zhong, W.; Li, G. Spatiotemporal-resolved protein networks profiling with photoactivation dependent proximity labeling. *Nat. Commun.* **2022**, *13*, 4906.
(13) Hananya, N.; Ye, X.; Koren, S.; Muir, T. W. A genetically encoded photoproximity labeling approach for mapping protein territories. *Proc. Natl. Acad. Sci. U. S. A.* **2023**, *120*, No. e2219339120.
(14) Engel, K. L.; Lo, H. G.; Goering, R.; Li, Y.; Spitale, R. C.; Taliaferro, J. M. Analysis of subcellular transcriptomes by RNA proximity labeling with Halo-seq. *Nucleic Acids Res.* **2022**, *50*, No. e24.
(15) Li, L.; Han, J.; Lo, H. G.; Tam, W. W. L.; Jia, H.; Tse, E. C. M.; Taliaferro, J. M.; Li, Y. Symmetry-breaking malachite green as a near-infrared light-activated fluorogenic photosensitizer for RNA proximity labeling. *Nucleic Acids Res.* **2024**, *52*, No. e36.
(16) Pan, C. R.; Knutson, S. D.; Huth, S. W.; MacMillan, D. W. C. microMap proximity labeling in living cells reveals stress granule disassembly mechanisms. *Nat. Chem. Biol.* **2025**, *21*, 490−500.
(17) Noma, K.; Jin, Y. Optogenetic mutagenesis in Caenorhabditis elegans. *Nat. Commun.* **2015**, *6*, 8868.
(18) Xu, X.; Muller, J. G.; Ye, Y.; Burrows, C. J. DNA-protein cross-links between guanine and lysine depend on the mechanism of oxidation for formation of C5 vs C8 guanosine adducts. *J. Am. Chem. Soc.* **2008**, *130*, 703−709.
(19) Ding, Y.; Fleming, A. M.; Burrows, C. J. Sequencing the Mouse Genome for the Oxidatively Modified Base 8-Oxo-7,8-dihydroguanine by OG-Seq. *J. Am. Chem. Soc.* **2017**, *139*, 2569−2572.
(20) Ren, Z.; Zhao, S.; Tang, W.; Zou, P. Spatially Resolved Multibait Mapping of Stress Granule and Processing Body Transcriptome. *Anal. Chem.* **2025**, *97*, 12767−12775.
(21) Hall, M. P.; Unch, J.; Binkowski, B. F.; Valley, M. P.; Butler, B. L.; Wood, M. G.; Otto, P.; Zimmerman, K.; Vidugiris, G.; Machleidt, T.; Robers, M. B.; Benink, H. A.; Eggers, C. T.; Slater, M. R.; Meisenheimer, P. L.; Klaubert, D. H.; Fan, F.; Encell, L. P.; Wood, K. V. Engineered luciferase reporter from a deep sea shrimp utilizing a novel imidazopyrazinone substrate. *ACS Chem. Biol.* **2012**, *7*, 1848−1857.
(22) Han, Y.; Branon, T. C.; Martell, J. D.; Boassa, D.; Shechner, D.; Ellisman, M. H.; Ting, A. Directed Evolution of Split APEX2 Peroxidase. *ACS Chem. Biol.* **2019**, *14*, 619−635.
(23) Cho, K. F.; Branon, T. C.; Rajeev, S.; Svinkina, T.; Udeshi, N. D.; Thoudam, T.; Kwak, C.; Rhee, H. W.; Lee, I. K.; Carr, S. A.; Ting, A. Y. Split-TurboID enables contact-dependent proximity labeling in cells. *Proc. Natl. Acad. Sci. U. S. A.* **2020**, *117*, 12143−12154.
(24) Boassa, D.; Lemieux, S. P.; Lev-Ram, V.; Hu, J.; Xiong, Q.; Phan, S.; Mackey, M.; Ramachandra, R.; Peace, R. E.; Adams, S. R.; Ellisman, M. H.; Ngo, J. T. Split-miniSOG for Spatially Detecting Intracellular Protein-Protein Interactions by Correlated Light and Electron Microscopy. *Cell Chem. Biol.* **2019**, *26*, 1407−1416.
(25) He, L.; Tan, P.; Zhu, L.; Huang, K.; Nguyen, N. T.; Wang, R.; Guo, L.; Li, L.; Yang, Y.; Huang, Z.; Huang, Y.; Han, G.; Wang, J.; Zhou, Y. Circularly permuted LOV2 as a modular photoswitch for optogenetic engineering. *Nat. Chem. Biol.* **2021**, *17*, 915−923.
(26) Lin, Z.; Schaefer, K.; Lui, I.; Yao, Z.; Fossati, A.; Swaney, D. L.; Palar, A.; Sali, A.; Wells, J. A. Multiscale photocatalytic proximity labeling reveals cell surface neighbors on and between cells. *Science* **2024**, *385*, No. eadl5763.
(27) Qu, D.; Li, Y.; Liu, Q.; Cao, B.; Cao, M.; Lin, X.; Shen, C.; Zou, P.; Zhou, H.; Zhang, W.; Pan, W. Photoactivated SOPP3 enables APEX2-mediated proximity labeling with high spatio-temporal resolution in live cells. *Cell Res.* **2025**, *35*, 149−152.
(28) Lee, A.; Sung, G.; Shin, S.; Lee, S. Y.; Sim, J.; Nhung, T. T. M.; Nghi, T. D.; Park, S. K.; Sathieshkumar, P. P.; Kang, I.; Mun, J. Y.; Kim, J. S.; Rhee, H. W.; Park, K. M.; Kim, K. OrthoID: profiling dynamic proteomes through time and space using mutually orthogonal chemical tools. *Nat. Commun.* **2024**, *15*, 1851.
(29) Qin, W.; Cheah, J. S.; Xu, C.; Messing, J.; Freibaum, B. D.; Boeynaems, S.; Taylor, J. P.; Udeshi, N. D.; Carr, S. A.; Ting, A. Y. Dynamic mapping of proteome trafficking within and between living cells by TransitID. *Cell* **2023**, *186*, 3307−3324.

https://doi.org/10.1021/acs.accounts.5c00390
Acc. Chem. Res. 2025, 58, 2526−2534